changes the energies and the agreement to experimental data for A1 and B by 1.5 kcal in energy and 10 Hz or less in the H1-H1′ dipolar splitting. The other splittings for A1 and B change by less than 8 Hz (Table IV). These changes are well within experimental error. Structure A2 relaxes to a structure that is energetically more favorable by 6 kcal but violates the H1-H1′ constraint by more than 20 Hz and the C2-H2 constraint by 9 Hz. Structure A2 can therefore be regarded as less probable based on either higher molecular energies or unacceptable deviations from experiment.

We believe procedures used in searching for preferred structures are reasonably robust. Initial searches for director axes with an assumed fixed conformation employ the same grid search algorithms used in the past.[5,6,10-12] The addition of molecular mechanics based minimization allows a moderately efficient extension of the search to cases in which conformational changes may have occurred. The fact that we see cases of displaced starting structures return to a common point suggests that we are approaching an adequate range of conformational search. The inclusion of a molecular mechanics minimization is also advantageous in cases where experimental data are too sparse to independently define a conformation. The molecular force field adds, in a systematic way, bonding constraints that are often implicit in choosing one conformation from experimental observations that give multiple solutions.[10-12,23]

Despite the increased data available from both deuterium and dipolar information, and the use of molecular mechanics constraints of allowed conformations, we are unable to distinguish structure A1 and B and define a single director orientation for trehalose. Energies for orientations A1 and B differ by less than 1 kcal with either high or low weights. All the experimental splittings are satisfied to within 0.25 of a typical line width even at low weights. It is interesting, however, that both the structures A1 and B1 have the same molecular conformation. Of all the geometries studied for each orientation only one geometry can satisfy the experimental constraints, and this geometry is nearly identical for both orientations A1 and B. Low-weight ϕ_H and ψ_Hs correspond to −61, −41 and −58, −44, respectively, while the internuclear distances, H1-H1′ are 2.9 and 2.8 Å, respectively. The two structures are shown in Figure 7. These are in agreement with the solution structure.[21] Deviations from the values seen in the two crystal structures are small, less than 5° in ϕ_H and 12° in ψ_H.[25,26] As suggested in our initial analysis of quadrupolar splittings, θs for the deuterium-labeled sites are close to 54 or 126°, causing the relatively small splittings. Order parameters of 0.02 are similar to those observed previously for sucrose and mannose.[4,5]

Acknowledgment. This research was supported by grants from the National Institutes of Health (GM 33225), and benefited from instrumentation provided through the shared instrumentation program of the Division of Research Resources of the National Institutes of Health (RR 02379).

Registry No. CsPFO, 17125-60-9; trehalose, 99-20-7.

Sulfur K-Edge X-ray Absorption Spectroscopy of Petroleum Asphaltenes and Model Compounds

Graham N. George and Martin L. Gorbaty*

Contribution from the Corporate Research Laboratories, Exxon Research and Engineering Company, Annandale, New Jersey 08801. *Received July 21, 1988*

Abstract: The utility of sulfur K-edge X-ray absorption spectroscopy for the determination and quantification of sulfur forms in petroleum asphaltenes has been investigated. Both X-ray absorption near edge structure (XANES) and extended X-ray absorption fine structure (EXAFS) spectra were obtained for a selected group of model compounds and for several petroleum asphaltene samples. For the model compounds the sulfur XANES was found to vary widely from compound to compound and to provide a fingerprint for the form of sulfur involved. The use of third derivatives of the spectra enabled discrimination of mixtures of sulfidic and thiophenic model compounds and allowed approximate quantification of the amount of each component in the mixtures and in the asphaltene samples. These results represent the first demonstration that nonvolatile sulfur forms can be distinguished and approximately quantified by direct measurement.

A major gap in our current knowledge of the chemistry of heavy hydrocarbons and coal concerns the chemical forms and quantities of organically bound sulfur in these materials. At best, current knowledge is qualitative and is based almost entirely upon characterization of volatile products. For coals, total organic sulfur is quantified by the difference between total and pyritic sulfur analyses. The different forms of sulfur have been assigned by a variety of methods, including mass spectroscopy of extractable materials and of liquid products, methyl iodide derivitization, catalytic decomposition, and oxidative techniques.[1] More recently, methods have been reported using a two-step chemical modification in conjunction with ^{13}C NMR spectroscopy to determine the chemical forms of sulfur in nonvolatile petroleum materials.[2] However, to date, no available method is completely adequate for directly determining both the forms and the amounts of organically bound sulfur in native coals and petroleum materials.

This report investigates the applications of X-ray absorption spectroscopy for the purpose of speciating and quantifying the forms of organic sulfur in solids and nonvolatile liquids. In earlier work Hussain et al.,[3] Spiro et al.,[4] and, later, Huffman et al.[5,6] demonstrated the potential of sulfur X-ray absorption spectroscopy in the qualitative determination of sulfur forms in coals; however, they made no attempt at quantification. Sulfur K-edge X-ray

(1) Van Krevelen, D. W. *Coal*; Elsevier: Amsterdam, 1961; p 171.
(2) Rose, K. D.; Francisco, M. A. *J. Am. Chem. Soc.* **1988**, *110*, 637.
(3) Hussain, Z.; Umbach, E.; Shirley, D. A.; Stohr, J.; Feldhaus, J. *Nucl. Instrum. Methods* **1982**, *195*, 115.
(4) Spiro, C. L.; Wong, J.; Lytle, F. W.; Greegor, R. B.; Maylotte, D. H.; Lamson, S. H. *Science* **1984**, *226*, 48.
(5) Huffman, G. P.; Huggins, F. E.; Shah, N.; Bhattacharyya, D.; Pugmire, R. J.; Davis, B.; Lytle, F. W.; Greegor, R. B. In *Processing and Utilization of High Sulfur Coals II*; Chugh, Y. P., Caudle, R. D., Eds.; Elsevier: Amsterdam, 1987; p 3.
(6) Huffman, G. P.; Huggins, F. E.; Shah, N.; Bhattacharyya, D.; Pugmire, R. J.; Davis, B.; Lytle, F. W.; Greegor, R. B. *ACS Div. Fuel Chem. Prep.* **1988**, *33*, 200.

0002-7863/89/1511-3182$01.50/0

absorption spectroscopy has also recently found applications in characterizing sulfur in several different biological systems.[7-10]

The approach taken in the present work was to examine the sulfur XANES[11] and EXAFS (extended X-ray absorption fine structure) spectra of organic compounds containing sulfur functionalities representative of those believed to be present in coals and heavy petroleum. The compounds investigated included mercaptans, sulfides, disulfides, and thiophenes. Compounds containing more oxidized forms of sulfur were also investigated, both for the sake of completeness and in order to explore the possibility of using sulfur X-ray absorption spectroscopy in conjunction with oxidative techniques for quantifying organically bound sulfur forms. Spectra were also obtained for three different petroleum asphaltene samples.

Experimental Section

Materials. All model compounds used in this study were obtained from Aldrich Chemical Co. and were used without further purification. The asphaltene samples were prepared from petroleum residua by precipitation from *n*-heptane following the procedure of Corbett.[12]

Sample Preparation. Solid samples were finely powdered and dusted onto mylar tape. In order to minimize thickness effects, some model compound samples were diluted with boron nitride. Liquid samples were prepared as a thin film sandwiched between two pieces of 6.3μm-thick polypropylene film.

Data Collection. Data were collected on samples at room temperature at the Stanford Synchrotron Radiation Laboratory on beam line VI-2 with the storage ring SPEAR running in dedicated mode (30–90 mA at 3 GeV). The 54-pole wiggler was operated in undulator mode with magnetic fields of 0.14–0.15 T, with a platinum-coated focusing mirror and using Si(111) or Ge(111) double-crystal monochromators. In order to ensure the maximum possible resolution, the aperture upstream of the mirror was reduced until the XANES spectrum of a sodium thiosulfate standard showed no further sharpening with subsequent reduction. Under these conditions we estimate upper limits for the resolution of approximately 0.5 and 0.9 eV when using Si(111) and Ge(111) monochromators, respectively. Because of its higher resolution, only the Si(111) monochromator was used for XANES measurements. In order to minimize atmospheric attenuation of the X-ray beam, the experimental apparatus was enclosed in a bag containing helium gas. X-ray absorption was monitored as the X-ray fluorescence excitation spectrum using a Stern–Heald–Lytle detector[13] or by measuring the total electron yield.[14] The energy scale was calibrated with reference to the lowest energy sulfur K-edge absorption peak of a sodium thiosulfate standard, assumed to be 2469.2 eV.[15] Although the absolute value for the energy calibration contains some uncertainty, the relative accuracy of the energy scale proved to be reproducible to within <0.1 eV.

Data Analysis. EXAFS spectra $\chi(k)$ were quantitatively analyzed by curve fitting to the following approximate expression:

$$\chi(k) \simeq \sum_{b} \frac{N_b A_b(k)}{kR_{ab}^2} e^{-2\sigma_{ab}^2 k^2} \sin\,[2kR_{ab} + \alpha_{ab}(k)]$$

where k is the photoelectron wavenumber, N_b is the number of b type atoms at a distance R_{ab} from the absorber atom a (in this case sulfur), σ_{ab} is the root mean square deviation of R_{ab} (the Debye–Waller factor), $A_b(k)$ is the total amplitude function, and $\alpha_{ab}(k)$ is the total phase shift function. For sulfur–carbon (S–C) interactions, values for the functions $\alpha(k)$ and $A(k)$ were obtained from the complex Fourier back-transform[16] of the first-shell Fourier-filtered EXAFS of dibenzothiophene, using 1.7404 Å for R_{ab}, taken from the crystal structure.[17] Because of this, values determined for the Debye–Waller factor for S–C interactions are quoted relative to this model as $\delta\sigma^2$. For sulfur–sulfur (S–S) interactions, theoretical values of $\alpha(k)$ and $A(k)$ were used[18] together with a linear amplitude scaling factor of 0.4, which was obtained by fitting the EXAFS of elemental sulfur.

Higher derivatives of XANES spectra were calculated with a cubic polynomial fit over a 0.4-eV range for each data point. In all cases

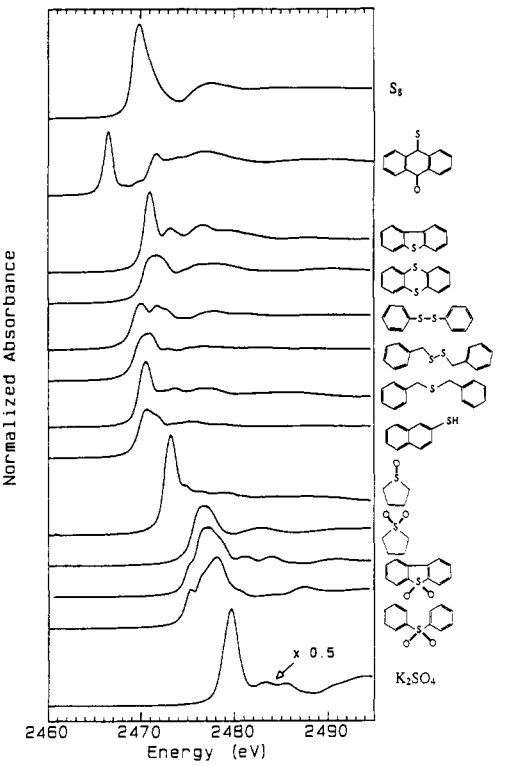

Figure 1. Sulfur K-edge XANES spectra and formulas of selected model compounds illustrating the diversity of sulfur XANES spectra. From top to bottom, elemental sulfur, thiohemianthraquinone, dibenzothiophene, thianthrene, diphenyl disulfide, dibenzyl disulfide, dibenzyl sulfide, 2-naphthalenethiol, tetramethylene sulfoxide, tetramethylene sulfone, dibenzothiophene sulfone, diphenyl sulfone, and potassium sulfate. All data have been normalized to the height of the edge jump. Because of the intensity of the spectrum of K_2SO_4, the vertical scale has been expanded by a factor of 2 in this case.

Table I. Sulfur K-Edge First Inflection Energies

compd	first inflection,[a] eV
K_2SO_4	2478.5
tetramethylene sulfone	2475.6
diphenyl sulfone	2474.8
dibenzothiophene sulfone	2474.7
tetramethylene sulfoxide	2472.4
2-methylthiophene	2470.6
benzothiophene	2470.4
dibenzothiophene	2470.4
methionine	2470.3
thianthrene	2470.2
dioctyl sulfide	2470.1
cystine	2470.1
tetramethylthiophene	2470.0
benzyl phenyl sulfide	2469.9
dibenzyl sulfide	2469.8
2-naphthalenethiol	2469.8
cysteine	2469.2
diphenyl disulfide	2469.2
dibenzyl disulfide	2469.1
sulfur	2469.1
thiohemianthraquinone	2466.1

[a] First inflection points were obtained from the position of the lowest energy maximum of the first derivative and are considered accurate to better than ±0.1 eV.

(7) Hedman, B.; Frank, P.; Penner-Hahn, J. E.; Roe, A. L.; Hodgson, K. O.; Carlson, R. M. K.; Brown, G.; Cerino, J.; Hettel, R.; Troxel, T.; Winick, H.; Yang, J. *Nucl. Instrum. Methods Phys. Res. Sect.* **1986**, *A246*, 797.
(8) Frank, P.; Hedman, B.; Carlson, R. M. K.; Tyson, T.; Roe, A. L.; Hodgson, K. O. *Biochemistry* **1987**, *26*, 4975.
(9) George, G. N.; Byrd, J.; Winge, D. R. *J. Biol. Chem.* **1988**, *263*, 8199.
(10) Hedman, B.; Frank, P.; Gheller, S. F.; Roe, A. L.; Newton, W. E.; Hodgson, K. O. *J. Am. Chem. Soc.* **1988**, *110*, 3798.
(11) X-ray absorption edge spectra and X-ray absorption near-edge spectra are referred to herein collectively as XANES.
(12) Corbett, L. W. *Anal. Chem.* **1969**, *41*, 576.
(13) Stern, E.; Heald, S. *Rev. Sci. Instrum.* **1979**, *50*, 1579.
(14) Purchased from the EXAFS Co., Seattle.
(15) Sekyama, H.; Kosugi, N.; Kuroda, H.; Ohta, T. *Bull. Chem. Soc. Jpn.* **1986**, *59*, 575.
(16) Eisenberger, P.; Shulman, R. G.; Kincaid, B. M.; Brown, G. S.; Ogawa, S. *Nature* **1978**, *274*, 30.
(17) Shaffrin, R. M.; Trotter, J. *J. Chem. Soc. A* **1970**, 1561.
(18) Teo, B. K.; Lee, P. A. *J. Am. Chem. Soc.* **1979**, *101*, 2815.

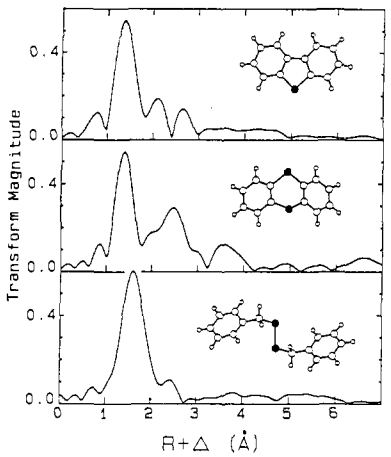

Figure 2. Sulfur EXAFS Fourier transforms of, from top to bottom, dibenzothiophene, thianthrene, and dibenzyl disulfide. The k range of the transforms was from 3 to 12 Å^{-1}, with k^3 weighting. The insets indicate the crystal structures of the compounds[17,20,21] (the darkened atoms correspond to sulfur, the largest light atoms to carbon, and the small light atoms to hydrogen).

spectra were normalized to the height of the edge jump, which was obtained by extrapolating the EXAFS spline function to the edge.

Results and Discussion

Model Compound XANES. Figure 1 compares the sulfur K-edge XANES of a number of model compounds. The XANES can be seen to vary widely from compound to compound. The first inflection energies of all compounds examined are given in Table I. As might be anticipated,[8,19] the first inflections of compounds with more oxidized sulfur are notably higher in energy than for those with reduced sulfur. The total span in energy is quite large, being some 12.4 eV between thiohemianthraquinone and potassium sulfate. Casual inspection of Figure 1 might suggest that the XANES from sulfur in different environments can be similar as, for example, with dibenzyl sulfide and dibenzothiophene. However, closer inspection (see also Table I) reveals that the edge of dibenzothiophene is displaced from that of dibenzyl sulfide, the first inflection energy being some 0.6 eV higher for the former compound. Much of the structure observed in XANES spectra corresponds to transitions to bound states, although other phenomena such as shake-up and shake-down satellites and continuum resonances[19] also contribute. Bound-state transitions commonly follow simple dipole selection rules, and an intense feature at a K edge would thus be expected to correspond to a transition to a level possessing significant p-orbital character (e.g., 1s $\rightarrow \pi^*$ or 1s $\rightarrow \sigma^*$). Although a detailed analysis of the XANES spectra in Figure 1 is outside the scope of this work, it is apparent that the spectra can readily be used as a fingerprint for the electronic nature of organically bound sulfur. Thus the sulfur XANES spectra of compounds with similar sulfur electronic environments were found to be similar. For example, dibenzothiophene and benzothiophene were found to give similar sulfur XANES spectra, whereas dibenzothiophene and thianthrene, which have significantly different environments, exhibit dissimilar sulfur XANES. It is a simple matter to distinguish between the forms of sulfur in the pure compounds investigated by simple examination of the sulfur XANES spectra.

EXAFS of Model Compounds and Asphaltene 1. We also examined the EXAFS spectra of a number of crystallographically characterized model compounds.[17,20,21] Figure 2 shows the EXAFS Fourier transform of dibenzothiophene, thianthrene, and dibenzyl disulfide. Both dibenzothiophene and thianthrene have the major Fourier transform peak at about $R + \Delta = 1.3$ Å, which is attributable to the first-shell carbon interactions, with S–C distances of 1.74 and 1.77 Å for dibenzothiophene and thianthrene, respectively.[17,20] More distant interactions with the aromatic ring carbons are also apparent in both transforms. For dibenzyl disulfide the major Fourier transform peak is at about $R + \Delta = 1.6$ Å and represents a mixture of first-shell sulfur and carbon interactions; no pronounced outer-shell interactions are apparent. Curve-fitting analysis of the model compound EXAFS (not illustrated) indicated that for first-shell interactions the systematic error in distance determinations was well within the usual EXAFS error of ±0.02 Å. The outer-shell interactions could also be reproduced by curve fitting, but with the much larger margin of uncertainty (ca. 0.1 Å) anticipated from the influence of multiple scattering effects (which are not included in our analysis).

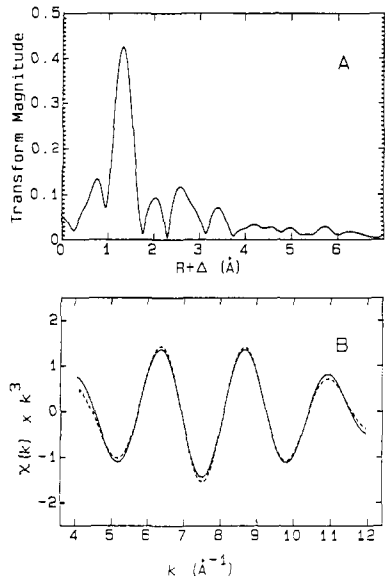

Figure 3. Sulfur EXAFS Fourier transform (A) and EXAFS curve-fitting analysis (B) of asphaltene sample 1. For A the k range was 3–12 Å^{-1}, with k^3 weighting. For B the data were Fourier filtered (k range = 3–13 Å^{-1}) to include first-shell interactions only (0.3-Å-width Gaussian window between 0.8 and 1.9 Å). The solid line indicates the Fourier-filtered data, and the broken line the best fit, which was calculated with $R_{ab} = 1.74$ Å and $\delta\sigma^2 = 0.0039$ Å^2.

EXAFS and XANES spectra of dibenzothiophene have previously been reported by Huffman et al.[5] The XANES spectrum presented by these workers differs in some respects from our data and most notably in possessing only a small peak at 2471 eV rather than the intense feature shown in Figure 1. This apparent discrepancy can readily be explained by noting the the XANES data presented by Huffman et al. are typical of spectra distorted by pronounced thickness effects, such as would be expected for a thick sample (ca. ≥0.1 mm) of pure compound, and we conclude that the differences between their data and ours are due to artifacts of sample preparation.

The EXAFS Fourier transform and the results of a first-shell fit to the EXAFS of asphaltene sample 1 (no EXAFS data for samples 2 and 3 were recorded) are shown in Figure 3, panels A and B, respectively. The EXAFS curve-fitting analysis indicates interactions from two carbon ligands, at a mean distance of 1.74 Å. It is clear from the S–C distance of 1.74 A that the bulk of the sulfur in the asphaltene sample is probably aromatic; indeed the similarity with the bond length for dibenzothiophene[10] is striking. However, the large value for $\delta\sigma^2$ of 0.0039 Å^2 indicates that there is probably some heterogeneity of bond lengths present. Several small outer-shell interactions in the asphaltene EXAFS are apparent from inspection of Figure 3A, with well-defined Fourier transform peaks at $R + \Delta = 2.1$, 2.7, and 3.4 Å. Inclusion of outer-shell interactions in a curve-fitting analysis of the unfiltered data did not yield completely satisfactory results. A marginally good fit was obtained, however, with S–C distances of 2.3 and 2.8 Å, although we do not view these results as sufficiently accurate to derive structural conclusions from them.

(19) Bianconi, A. In *X-ray Absorption*; Koningsberger, D. C., Prins, R., Eds.; Wiley: New York, 1988; p 573.
(20) Larson, S. B.; Simonsen, S. H.; Martin, G. E.; Smith, K.; Puig-Torres, S. *Acta Crystallogr.* **1984**, *B40*, 103.
(21) Lee, J. D.; Bryant, M. W. R. *Acta Crystallogr.* **1969**, *B25*, 2497.

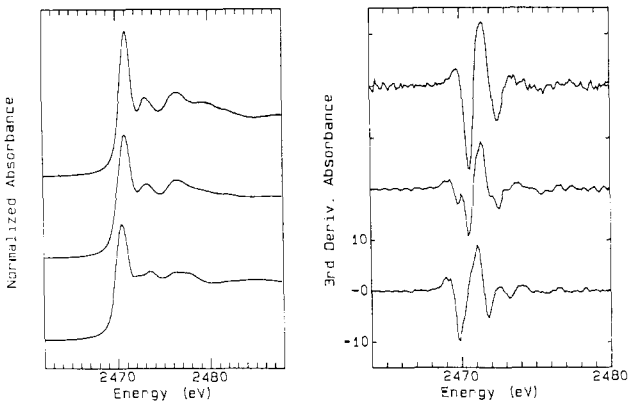

Figure 4. Sulfur XANES spectra of mixed dibenzothiophene and dibenzyl sulfide. The left panel shows the absorption spectra, and the right panel the corresponding third derivatives. From top to bottom, pure dibenzothiophene, a 1:1 molar mixture of dibenzothiophene and dibenzyl sulfide, and pure dibenzyl sulfide.

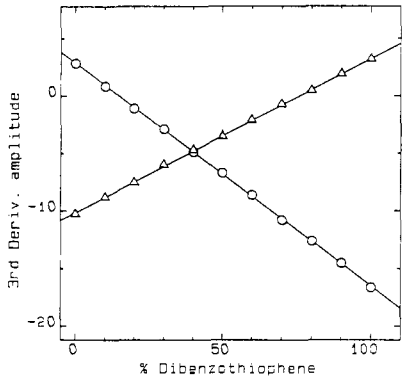

Figure 5. Calibration plot for quantification of dibenzothiophene and dibenzyl sulfide mixtures from computer-generated mixtures of the pure compound. Points denoted as (Δ) indicate the third-derivative amplitude at 2469.8 eV, and those as (O) the third-derivative amplitude at 2470.8 eV.

XANES of Mixtures of Model Compounds and of Asphaltenes. To address the question of whether sulfur XANES spectra can be used to distinguish and quantify different sulfur forms in mixtures, spectra were collected of mixtures of dibenzothiophene and dibenzyl sulfide. Illustrative sulfur XANES spectra for the pure compounds and a 1:1 molar mixture are shown in Figure 4, together with the corresponding third-derivative spectra. Although the absorption line shapes in Figure 4 all appear very similar, significant differences are revealed by the third derivatives. Because of this it proved possible to identify each compound in the presence of the other. Additionally by simply measuring the heights of the third-derivative features at 2469.8 and 2470.8 eV, an approximate estimate of the amounts of each component can be obtained. A calibration plot for this purpose is illustrated in Figure 5.

Sulfur XANES spectra and the corresponding third-derivative spectra of three asphaltene samples are shown in Figure 6. Even casual inspection of the figure shows that, while the absorption line shapes look quite similar, the third derivatives show clear differences. By comparison with the model compound data, and in agreement with the EXAFS results discussed above, we conclude that the organic sulfur bound in asphaltene sample 1 consists almost entirely of dibenzothiophenic forms. The sulfur of samples 2 and 3, however, appears to be mixtures of thiophenic and sulfidic forms (note the absence of the sulfide peak at 2469.8 eV in the spectrum of sample 1 and the appearance of this feature in the other two). This conclusion is consistent with pyrolysis data for these asphaltene samples, which yield larger quantities of hydrogen sulfide from samples 2 and 3 relative to sample **1**. Aliphatic and aryl alkyl sulfides are known to produce hydrogen sulfide on thermal decomposition.[22]

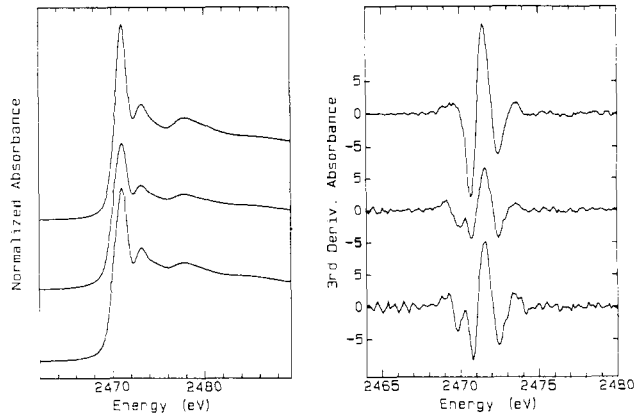

Figure 6. Sulfur XANES spectra of asphaltenes. The left panel shows the absorption spectra, and the right panel the corresponding third derivatives, from top to bottom, samples 1, 2, and 3.

Assuming that the composition of the sulfur forms in the asphaltene samples is approximated by the simple two-component mixture of dibenzothiophene and dibenzyl sulfide models, we can obtain an estimate of the relative molar quantities of sulfidic and thiophenic forms as described above and from Figure 5. This simple analysis indicates that sample 3 contains about 50% sulfidic forms and 50% thiophenic forms (i.e., about a 1:1 molar mixture), while sample 2 contains 43% sulfidic and 37% thiophenic. In the latter case, the totals do not add to 100%. For X-ray fluorescence data this method of quantification is susceptible to errors resulting from distortion of the XANES spectra by the thickness effects. For accurate quantification care must be taken, especially for model compounds, by diluting the samples sufficiently to ensure that minimal thickness effects occur. An alternative strategy is to employ electron yield rather than X-ray fluorescence detection, and this was done for some of the model compound data of Figure 1 (i.e., elemental sulfur and K_2SO_4). Note that even with optimal grinding, thickness effects are difficult to completely eliminate by dilution with boron nitride, and some of the spectra in Figure 1 may still exhibit residual distortion. Such thickness effects may be indicated for sample 2 by the low values for both sulfur forms determined above, although because of the dilute nature of this sample we consider this unlikely. A more probable explanation is that a range of slightly different sulfur types, of both sulfidic and thiophenic forms, causes a broadening of the features of the XANES spectrum. In agreement with this the structure of the third-derivative spectrum of sample 2 does appear to be broadened relative to that of the spectrum of sample 3 in Figure 6.

Despite the overall similarity between the XANES spectrum of the mixed model compounds and the asphaltene samples, there are, however, some significant differences in the relative energies of the various features. One possible explanation for these differences is that subtle electronic differences at the sulfur are reflected in the sulfur XANES. Such differences might be expected to arise from extended ring structures or from substituents. This will be a subject for further study.

Conclusions

This work has demonstrated for the first time that organically bound sulfur forms can be distinguished and in some manner quantified in model compound mixtures and in petroleum asphaltenes. The use of the third-derivative XANES spectra was the critical factor in allowing this analysis. The tentative quantitative identifications of sulfur forms are consistent with the chemical behavior of the asphaltene samples. Further work is in progress to extend these techniques to other nonvolatile and solid hydrocarbon materials.

Acknowledgment. X-ray absorption spectra were recorded at the Stanford Synchrotron Radiation Laboratory, which is funded by the Department of Energy under Contract DE-AC03-82ER-

(22) Fromm, E.; Achert, O. *Ber.* **1903**, *36*, 545.

13000, Office of Basic Energy Sciences, Division of Chemical Sciences, and the National Institutes of Health, Biotechnology Resource Program, Division of Research Resources. We thank Drs. M. K. Eidsness and S. P. Cramer for their assistance with early experiments.

Registry No. S, 7704-34-9; K_2SO_4, 7778-80-5; tetramethylene sulfone, 126-33-0; diphenyl sulfone, 127-63-9; dibenzothiophene sulfone, 1016-05-3; tetramethylene sulfoxide, 1600-44-8; 2-methylthiophene, 554-14-3; benzothiophene, 95-15-8; dibenzothiophene, 132-65-0; methionine, 63-68-3; thianthrene, 92-85-3; dioctyl sulfide, 2690-08-6; tetramethylthiophene, 14503-51-6; benzyl phenyl sulfide, 831-91-4; 2-naphthalenethiol, 91-60-1; cysteine, 52-90-4; diphenyl disulfide, 882-33-7; thiohemianthraquinone, 68629-85-6.

Equilibrium Dynamics in the Thallium(III)–Chloride System in Acidic Aqueous Solution

Istvan Banyai[1] and Julius Glaser*

Contribution from The Royal Institute of Technology (KTH), Department of Inorganic Chemistry, S-100 44 Stockholm, Sweden. *Received August 9, 1988*

Abstract: Kinetics of ligand exchange in the thallium(III)–chloride system in aqueous three molar perchloric acid solution was studied by measuring ^{205}Tl NMR line widths at 25 °C. The rate constants for the reactions

$$TlCl_m^{3-m} + {}^*TlCl_n^{3-n} \underset{}{\overset{k_{mn}}{\rightleftharpoons}} {}^*TlCl_m^{3-m} + TlCl_n^{3-n}$$

are $k_{01} = 4.5 \times 10^4$ (7.8×10^3 at 0 °C), $k_{12} = 5.2 \times 10^4$ (1.5×10^4), $k_{23} = 2.7 \times 10^7$ (3.3×10^6), $k_{34} < 3 \times 10^7$ M^{-1} s^{-1}; for the reaction

$$Tl^{3+} + TlCl_2^+ \underset{}{\overset{k_{02}}{\rightleftharpoons}} 2TlCl^{2+}$$

$k_{02} = 6.4 \times 10^5$ M^{-1} s^{-1} (1.7×10^5), and for the anation reactions

$$TlCl_n^{3-n} + Cl^- \underset{}{\overset{k'_{n(n+1)}}{\rightleftharpoons}} TlCl_{n+1}^{2-n}$$

$k'_{01} < 1 \times 10^8$, $k'_{12} = 3.3 \times 10^8$ (2.4×10^8), $k'_{23} = 1.3 \times 10^9$, and $k'_{34} = 4.7 \times 10^8$ M^{-1} s^{-1}. The first type of exchange dominates at low chloride to thallium ratios (Cl_{tot}/Tl_{tot}) = $R \leq 2$, the second type is only observed when the species Tl^{3+} and $TlCl_2^+$ are present, whereas the third one dominates at all higher R values. The activation parameters for the reaction represented by k_{01} are $\Delta H^\ddagger = 49$ (±2) kJ mol^{-1} and $\Delta S^\ddagger = +12$ (±0.3) J mol^{-1} K^{-1}. A mechanism for this reaction is suggested to be a dissociatively activated interchange process. The activation parameters for the reaction represented by k'_{34} are $\Delta H^\ddagger = 6.6$ kJ mol^{-1} and $\Delta S^\ddagger = -107$ J mol^{-1} K^{-1}. An associatively activated interchange mechanism for this reaction is proposed. The stability constant for the complex $TlCl_5^{2-}$ was estimated to be $K_5 = [TlCl_5^{2-}]/\{[TlCl_4^-][Cl^-]\} \approx 0.5$ M^{-1}.

The complexes formed in the thallium(III)–chloride system are among the strongest metal-ion–chloride complexes, and their equilibria have been extensively studied.[2-8] There is information on their structures both in solid and in solution.[9-13] However, there are only a few results on the kinetics of the complex formation and ligand exchange reactions of the thallium(III) ion.[14-17] The reason is probably that these reactions are rather fast not only on the traditional kinetic time scale but also on the NMR time scale of common NMR nuclei, e.g., ^1H or ^{35}Cl.[16]

Although there is a lot of data for the ligand and solvent exchange for the octahedral three-valent metal ions,[18] an investigation of dynamics in the thallium(III)–chloride system seems to be interesting. Structural studies showed that the geometry of thallium–halide complexes is different depending on the number of coordinated ligands.[12,13] In aqueous solution the aquated thallium(III) ion, the pentaaqua monochloro, and tetraaqua dichloro complexes are probably octahedral, the trichloro complex is tetrahedral or trigonal bipyramidal or both in equilibrium, but the fourth complex is clearly tetrahedral. These changes in the structure should influence the ligand exchange kinetics.

In the case of Al^{3+}, Ga^{3+}, and In^{3+} the mechanism of solvent exchange shows a trend to turn from a dissociatively into associatively activated process when the ionic radius increases.[19] Although the mechanism of solvent exchange is sometimes different from the mechanism of ligand exchange, in many cases similar trends have been observed. Kawai et al. studied the complex formation between Ga^{3+}, In^{3+}, and Tl^{3+} and semi-xylenol orange[14] and later between Tl^{3+} and 4-(2-pyridylazo)resorcinol,[15] by stopped-flow technique and found that the second-order rate

(1) Permanent address: Department of Physical Chemistry, Lajos Kossuth University, H-4010 Debrecen, Hungary.
(2) Lee, A. G. *The Chemistry of Thallium*; Elsevier: Amsterdam, 1971; pp 44–91, and references therein.
(3) Ahrland, S.; Grenthe, I.; Johansson, L.; Noren, B. *Acta Chem. Scand.* **1963**, *17*, 1567.
(4) Ahrland, S.; Johansson, L. *Acta Chem. Scand.* **1964**, *18*, 2125.
(5) Woods, M. J. M.; Gallagher, P. K.; Hugus, Z. Z.; King, E. L. *Inorg. Chem.* **1964**, *3*, 1313.
(6) Kul'ba, F. Y.; Mironov, V. E.; Mavrin, I. F. *Zh. Fiz. Khim.* **1965**, *39*, 2595.
(7) Glaser, J.; Biedermann, G. *Acta Chem. Scand.* **1986**, *A40*, 331.
(8) Glaser, J.; Henriksson, U. *J. Am. Chem. Soc.* **1981**, *103*, 6642.
(9) Davies, E. D.; Long, D. A. *J. Chem. Soc. A* **1968**, 2050.
(10) Biedermann, G.; Spiro, T. G. *Chem. Scr.* **1971**, *1*, 155.
(11) (a) Spiro, T. G. *Inorg. Chem.* **1965**, *4*, 731. (b) *Ibid.* **1967**, *6*, 569.
(12) Glaser, J.; Johansson, G. *Acta Chem. Scand.* **1982**, *A36*, 125.
(13) Glaser, J. *Acta Chem. Scand.* **1982**, *A36*, 451.
(14) Kawai, Y.; Takahashi, T.; Hayashi, K.; Imamura, T.; Nakayama, H.; Fujimoto, M. *Bull. Chem. Soc. Jpn.* **1972**, *45*, 1417.
(15) Funada, R.; Imamura, T.; Fujimoto, M. *Bull. Chem. Soc. Jpn.* **1979**, *52*, 1535.
(16) Lincoln, S. F.; Sandercock, A. C.; Stranks, D. R. *Aust. J. Chem.* **1975**, *28*, 1901.
(17) Henriksson, U.; Glaser, J. *Acta Chem. Scand.* **1985**, *A39*, 355.
(18) Wilkins, R. G. *The Study of Kinetics and Mechanism of Reactions in Transition Metal Complexes*; Allyn and Bacon: Boston, 1974.
(19) van Eldik, R. *Inorganic High Pressure Chemistry Kinetics and Mechanisms*; Elsevier: Amsterdam, 1986.

0002-7863/89/1511-3186$01.50/0